ZnO Nanoparticles Synthesized Using Glycosmis pentaphylla: A Green Approach to Antimicrobial Activity

Sreela S Nair[1], S. Rubila[2] , P. Prakash, V. Balaprakash[1*], K. Thangavel[1]
[1]Department of Electronics, Hindustan College of Arts and Science, Coimbatore, Tamil Nadu, India-641028.
[2]Department of Plant Molecular Biology and Bioinformatics, Tamilnadu Agricultural University, Coimbatore-641003, Tamilnadu, India
[3]Department of Physics, Suguna College of Engineering, Coimbatore, Tamilnadu, India

Corresponding Author: (V. Balaprakash)
vbalaprakash24@gmail.com

Abstract:

ZnO nanoparticles derived from *Glycosmis pentaphylla* have been utilized for antimicrobial purposes for a long time. These nanoparticles have garnered significant interest, as the demand for nanotechnology continues to grow due to their diverse applications. The co-precipitation method, using varying ratios of 20 ml, 40 ml, and 60 ml of plant extract, is preferred for synthesizing ZnO nanoparticles because of its high efficiency, low production cost, and environmental sustainability. The synthesized nanoparticles are aimed at targeting pathogenic microorganisms, including bacteria such as *E. coli* and *Staphylococcus aureus*, and fungi like *Candida albicans* and *Aspergillus flavus*.

The ZnO nanoparticles were analyzed for their crystal structure, morphology, and optical properties using techniques such as X-ray diffraction, scanning electron microscopy, UV-visible spectroscopy, and Fourier-transform infrared spectroscopy. The ZnO structures obtained exhibited high crystallinity and strong emission peaks, especially with the 60 ml ratio of *Glycosmis pentaphylla* extract. This study demonstrates that ZnO nanoparticles have superior antimicrobial activity against both bacterial and fungal pathogens when compared to microparticles, largely due to their increased specific surface area. The higher concentrations of ZnO nanoparticles show a marked enhancement in antimicrobial activity, as highlighted in this paper.

Key words:Glycosmis pentaphylla, ZnO nanoparticles, X-ray diffraction, Scanning Electron Microscope, FTIR, Antimicrobial activity.

Introduction:

Nanotechnology has emerged as a pivotal field in the 21st century, particularly in biomedical and pharmaceutical industries, where the development of novel plant-based nanomaterials for drug formulation is highly anticipated [1]. Green synthesis of nanoparticles using plant extracts has gained prominence due to its cost-effectiveness and non-polluting nature, making it an attractive

alternative to traditional physical and chemical synthesis methods [2]. The growing population and increasing prevalence of diseases have sparked research into biological activities, leading to the development of new materials aimed at combating these health challenges. These new nanomaterials, with unique properties, are highly sought after in materials science and biology.

The production of nanomaterials through simple, low-cost approaches is a significant area of focus for researchers. The properties of these nanomaterials—such as phase composition, crystalline structure, size, dispersion, and morphology—play a crucial role in their applications in optics, photonics, sensors, and solar cells, enabling the creation of high-quality devices. Organic antibacterial compounds tend to be unstable in nature, but when combined with inorganic metals or metal oxides, they become more effective at targeting a range of pathogens [3-5]. Among metal oxides, ZnO has attracted particular attention for its role as an antimicrobial agent. ZnO has been shown to reduce the adhesion of *Escherichia coli* to intestinal cells [6]. A promising antimicrobial agent must exhibit selective toxicity towards targeted microbes, and ZnO nanoparticles have demonstrated potent bactericidal and fungicidal activity against specific pathogens [7-9].

While the complete mechanism of antibacterial activity for ZnO nanoparticles is not fully understood, several studies suggest that ZnO NPs can disrupt microbial cell membranes, leading to loss of integrity, functional instability, and ultimately bacterial death [10]. Other studies have highlighted that ZnO NPs can interfere with bacterial DNA, membrane proteins, and disrupt bacterial growth and reproduction [11,12]. Green synthesis of ZnO nanoparticles from natural sources, such as plants and microorganisms, has garnered attention due to the challenges associated with managing cell cultures. Additionally, plant-mediated synthesis of nanoparticles offers the potential for large-scale production [13,14].

Glycosmis pentaphylla, a plant with medicinal properties traditionally used in Bangladesh, has not been extensively studied despite its historical use for various ailments [15]. This study focuses on investigating the antimicrobial properties of *Glycosmis pentaphylla* against bacterial and fungal pathogens. Plants like *Glycosmis pentaphylla* contain essential secondary metabolites such as flavonoids, saponins, tannins, alkaloids, steroids, phenols, glycosides, and sugars, which enhance their antibacterial properties against pathogens, including gram-negative bacteria like *E. coli* and *Staphylococcus aureus* [16,17].

E. coli is a gram-negative bacterium responsible for a variety of diseases, including urinary tract infections, sepsis, neonatal meningitis, and more. It can also cause opportunistic infections like osteomyelitis, wound infections, and cellulitis [18,19]. *Staphylococcus aureus* is a significant pathogen causing diseases like osteoarticular infections, skin diseases, pleuropulmonary infections, and endocarditis. The rise of drug-resistant *Staphylococcus aureus* has created challenges in clinical settings, making phytomedicine a promising alternative [20]. *Candida albicans* is a fungus commonly found in the alimentary canal and mucosal areas of the human body, capable of causing life-threatening infections, particularly in immuno compromised individuals. Another important fungal pathogen is *Aspergillus flavus*, which can lead to diseases such as asthma, mycotic keratitis, and wound infections [21].

Metal oxide nanoparticles, including ZnO, have attracted interest for their antimicrobial activity due to their wide band gap energy, which increases as particle size decreases. One-dimensional materials (1D) have higher specific surface areas, allowing for faster electron transport, making them ideal for various applications. ZnO nanoparticles, in particular, are favored due to their high refractive index, strong optical absorption, and antimicrobial properties, which help in combating both pathogenic and spoilage microorganisms. Their antimicrobial action is attributed to the generation of reactive oxygen species, membrane disruption, and the release of antimicrobial ions (Zn^{2+}) [23].

The U.S. Food and Drug Administration (FDA) classifies ZnO as a Generally Recognized as Safe (GRAS) substance, further supporting its potential for use in antimicrobial applications [23]. The growing concern over antibiotic resistance has spurred interest in novel antimicrobial agents, with metal oxide nanoparticles like ZnO showing great promise. In this study, the antimicrobial activity of ZnO nanoparticles synthesized using the co-precipitation method with *Glycosmis pentaphylla* extract was evaluated. The nanoparticles were characterized by X-ray diffraction, scanning electron microscopy, UV-visible spectroscopy, and Fourier-transform infrared spectroscopy. Antifungal activity was also assessed against *Candida albicans* and *Aspergillus flavus*, with the minimum inhibitory concentration (MIC) values compared to the standard antibiotic kanamycin.

This research highlights the potential of ZnO nanoparticles as effective antimicrobial agents, capable of targeting both bacterial and fungal pathogens through their unique properties and mechanisms of action.

2. MATERIALS AND METHOD:

2.1. Materials:

Zinc nitrate hexahydrate ($Zn(NO_3)_2.6H_2O$), distilled water, Whatman's filter, were purched from scientific centre at Coimbatore. The Glycosmis pentaphylla leaves were collected from our college surrounding.

2.2. Preparation of extract:

10g of plant powder was placed in round bottom flask containing 100 ml deionized water and maintained under 50-60°C temperature for 30 minutes. Later, the solution was allowed to cool at room temperature, filtered through Whatman's filter paper no. 1. Beyond filtering, the aqueous plant extract was obtained and stored at 4 °C, which was further used in the synthesis of nanoparticles.

Figure.1: Image of Glycosmis pentaphylla

2.3. Synthesis of Zinc Oxide nanoparticles by co-precipitation method

Pure zinc oxide (ZnO) nanoparticles were synthesized using the co-precipitation method with varying concentrations of plant extract (20 ml, 40 ml, and 60 ml) as detailed in reference [21]. To begin, 20 ml of aqueous Glycosmis pentaphylla plant extract was taken in a round-bottom flask and stirred at 70°C for 20 minutes. Subsequently, 0.1 ml of 3M zinc nitrate hexahydrate ($Zn(NO_3)_2 \cdot 6H_2O$) was added to the solution while maintaining continuous stirring. The resulting precipitate, which contained the pure compound, was separated by centrifugation to remove the supernatant, with ethanol used for washing. The collected material was dried in a hot air oven at 60°C for 10 hours.

For the synthesis involving 40 ml and 60 ml of plant extract, the process was slightly modified. The respective volumes of plant extract (40 ml and 60 ml) were taken in separate beakers, heated, and stirred at 70°C for 15 minutes. To each beaker, 0.1 ml of 3M zinc nitrate hexahydrate ($Zn(NO_3)_2 \cdot 6H_2O$) was gradually added. The precipitates formed in each case were centrifuged to

separate the supernatant, thoroughly washed multiple times with distilled water and once with ethanol, and then dried in a hot air oven at 60°C for 12 hours.

Figure.2: Extraction of Glycosmis plant

Synthesis of pure Zinc Oxide nanoparticles by co-precipitation method

A color changes from yellow to brown in the reaction mixture indicating the formation of ZnO-NPs. The intensity (Light to dark) of the color is directly proportional to the concentration of plant extract added (Figure 3 and 4).

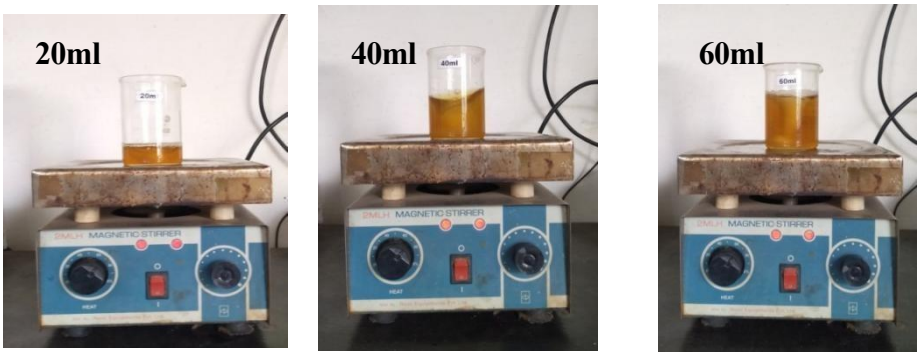

Figure.3: Synthesis of pure Zinc Oxide nanoparticles by co-precipitation method.

20ml **40ml** **60ml**

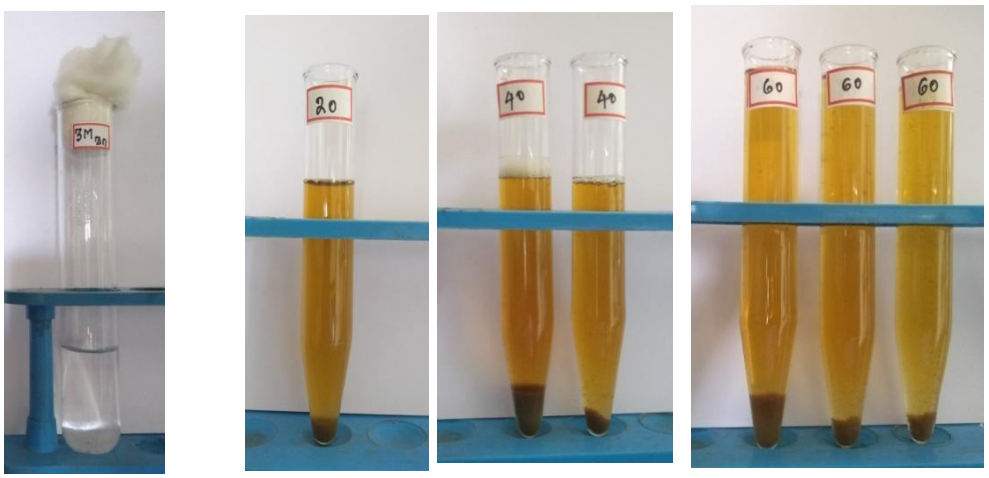

Figure 4. Images of Centrifugation and Collection of ZnO-NPs solution using Glycosmis leaf extract

2.3. Determination of antimicrobial activity

The antimicrobial activity was evaluated using the disc diffusion method, as outlined by NCCLS (1993) [22]. For this assay, antibiograms were prepared using the disc diffusion technique with the test samples. Petri dishes were set up by pouring 30 ml of nutrient agar (NA) medium for bacterial strains and potato dextrose agar (PDA) medium for fungal strains. The test organisms were inoculated onto the solidified agar plates using a micropipette, spread evenly, and allowed to dry for 10 minutes.

The media surfaces were inoculated with bacterial and fungal cultures derived from 24-hour and 48-hour broth cultures, respectively. Sterile cotton swabs were dipped into standardized suspensions of bacterial or fungal test organisms and used to evenly spread the inoculum across the surfaces of NA plates for bacteria and PDA plates for fungi.

The bacterial strains tested included *Escherichia coli* (MTCC 732) and *Staphylococcus aureus* (MTCC 3160), while the fungal strains included *Candida albicans* (MTCC 183) and *Aspergillus flavus* (MTCC 10180). Sterile filter paper discs (6 mm diameter) were impregnated with varying concentrations of *Glycosmis pentaphylla*-mediated ZnO nanoparticles (50 µl, 100 µl, and 200 µl) and placed onto the agar plates using sterile forceps. A standard solution (30 µl) was also applied as a positive control (Chloramphenicol for bacteria and Fluconazole for fungi).

The inoculated plates were incubated at 37°C for 24 hours for bacterial strains and 48 hours for fungal strains. Every experiment was performed in triplicate for ensuring accuracy and reproducibility.

2.4. Characterization Technique:

The structural characterization of ZnO nanoparticles was performed using X-ray diffraction (XRD) analysis on an X'Pert Pro diffractometer, utilizing Cu Kα radiation with a wavelength of 1.5418 Å and angular resolution. The particle size and morphology of the nanoparticles were examined using a ZEISS scanning electron microscope (SEM) operating under a vacuum of approximately 10^{-5} torr and at an accelerating voltage of 10 kV. The particle sizes were further analyzed using the ImageJ magnification software compatible with SEM data.

To identify functional groups, energy-dispersive X-ray spectroscopy (EDS) attached to the SEM was employed. Optical properties of the silver nanoparticles were studied using a Perkin Elmer photometer, scanning wavelengths between 200–900 nm to detect characteristic peaks.

Fourier transform infrared (FTIR) spectroscopy was conducted using a spectrophotometer to identify functional groups and their characteristic peaks within the range of 400–4000 cm^{-1}. Both UV-visible spectroscopy and FTIR techniques were used to note and confirm peak values.

The antimicrobial activity was assessed through the disc diffusion method, following the NCCLS guidelines.

3. Result and Discussion:

3.1. XRD pattern of ZnO-NPs

X-ray diffraction (XRD) is widely utilized to identify the chemical composition and crystal structure of materials. The XRD patterns of ZnO nanoparticles synthesized using three different extract ratios via the co-precipitation method are presented in Figure 5. The biosynthesized ZnO nanoparticles exhibited well-defined crystalline peaks, as shown in the figure. The diffraction peaks observed at 2θ values of approximately 31.66°, 34.45°, 36.55°, 47.53°, 56.49°, and 62.70°

correspond to the (100), (002), (101), (102), (110), and (103) crystal planes, respectively. These results align with findings from previous studies [29-31].

All diffraction peaks were accurately indexed and compared with the standard JCPDS file card No. 36-1451, confirming the hexagonal structure of the ZnO nanoparticles synthesized with varying extract ratios. The results suggest that increasing the extract ratio enhances the intensity of the peaks, which correlates with an increase in particle size. This phenomenon may be attributed to nucleation or crystal growth, as well as the incorporation of the plant extract into the lattice structure [31].

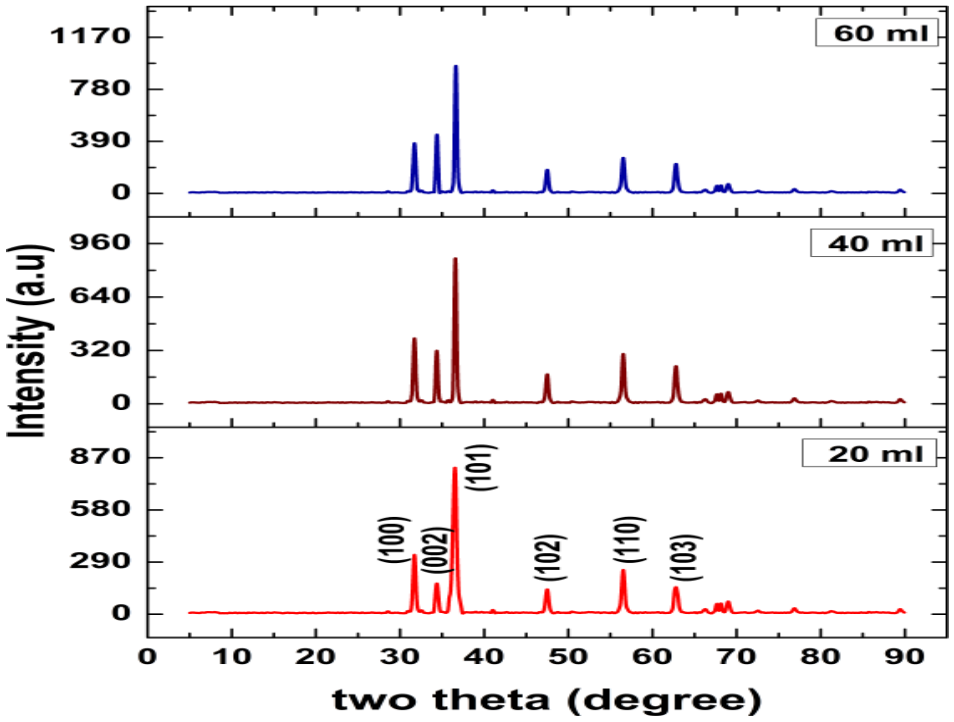

Figure .5: XRD patterns of ZnO NPs synthesized using Zinc nitrate hexahydrate and extract of different ratios by volume (20, 40 and 60ml)

Table. 1: Structural parameter of ZnO nanoparticles with various concentration of extraction(20,40,60 ml)

Extraxt ratio(ml)	2θ (degree)	lattice parameters			D (nm)	Dislocation density (δ) $(nm^2)^{-1}$ $(\times 10^{15})$	Micro strain (ε)	Stacking Fault
		a=b (Å)	c(Å)	Volume				

							(lines m^{-2})	
20	36.55	3.2478	5.200	47.503	10.17	0.087	0.065	0.062
40	36.58	3.2447	5.197	47.387	14.41	0.072	0.032	0.049
60	36.62	3.2492	5.204	47.584	18.07	0.004	0.025	0.173

3.2. SEM and EDAX Analysis

The surface morphology of ZnO nanoparticles synthesized with different extract concentrations (20 ml, 40 ml, and 60 ml) was analyzed using scanning electron microscopy (SEM). The SEM micrographs, shown in Figure 6, reveal that the majority of the synthesized nanoparticles exhibit a spherical shape across all concentrations. The corresponding histograms of the SEM analysis for the three extract concentrations are also displayed in Figure 6.

The analysis indicates that the nanoparticles formed through the aggregation of spherical particles exhibit a range of sizes. For the 20 ml extract, the sizes ranged from 11 to 50 nm, with an average size of 31.41 nm. Similarly, for the 40 ml extract, the nanoparticles were polydispersed, with sizes varying between 30 and 80 nm and an average size of 55.46 nm. For the 60 ml extract, the particles were more scattered, with sizes ranging from 44 to 102 nm and an average size of 73.02 nm.

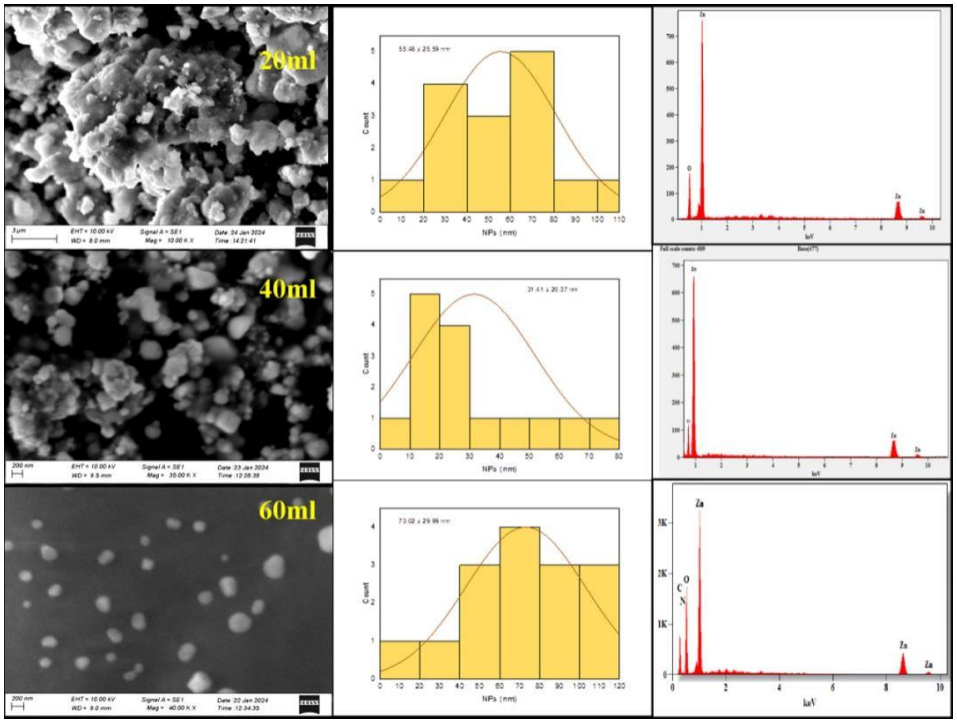

Figure 6. Scanning electron microscope image, histogram of zinc oxide nanoparticles, and EDAX spectra of various concentration of extracts (20ml,40ml and 60ml)

The elemental composition of the biosynthesized nanomaterials was analyzed using energy-dispersive X-ray (EDX) spectroscopy. The EDX spectra confirmed the presence of zinc as a key component, highlighting the successful synthesis and purity of zinc oxide nanoparticles derived from plant extracts. Elemental analysis was performed for nanoparticles synthesized using extract volumes of 20 ml, 40 ml, and 60 ml.The results revealed variations in elemental composition based on extract concentration. For the 20 ml extract, the highest proportions of zinc and oxygen by weight were 48.14% and 51.86%, respectively. With the 40 ml extract, zinc content increased to 63.67%, while oxygen content decreased to 36.33%. In contrast, for the 60 ml extract, the composition included zinc (11.71%), oxygen (51.09%), carbon (29.66%), and nitrogen (7.55%) (Figure 6).

These findings indicate that as the extract concentration increased, the zinc content decreased, while the proportions of oxygen, carbon, and nitrogen associated with phytochemical components showed an increasing trend.

3.3. HRTEM analysis:

The elemental composition of the biosynthesized nanomaterials was analyzed using energy-dispersive X-ray (EDX) spectroscopy. The EDX spectra confirmed the presence of zinc as a key

component, highlighting the successful synthesis and purity of zinc oxide nanoparticles derived from plant extracts. Elemental analysis was performed for nanoparticles synthesized using extract volumes of 20 ml, 40 ml, and 60 ml.The results revealed variations in elemental composition based on extract concentration. For the 20 ml extract, the highest proportions of zinc and oxygen by weight were 48.14% and 51.86%, respectively. With the 40 ml extract, zinc content increased to 63.67%, while oxygen content decreased to 36.33%. In contrast, for the 60 ml extract, the composition included zinc (11.71%), oxygen (51.09%), carbon (29.66%), and nitrogen (7.55%) (Figure 6).These findings indicate that as the extract concentration increased, the zinc content decreased, while the proportions of oxygen, carbon, and nitrogen associated with phytochemical components showed an increasing trend.

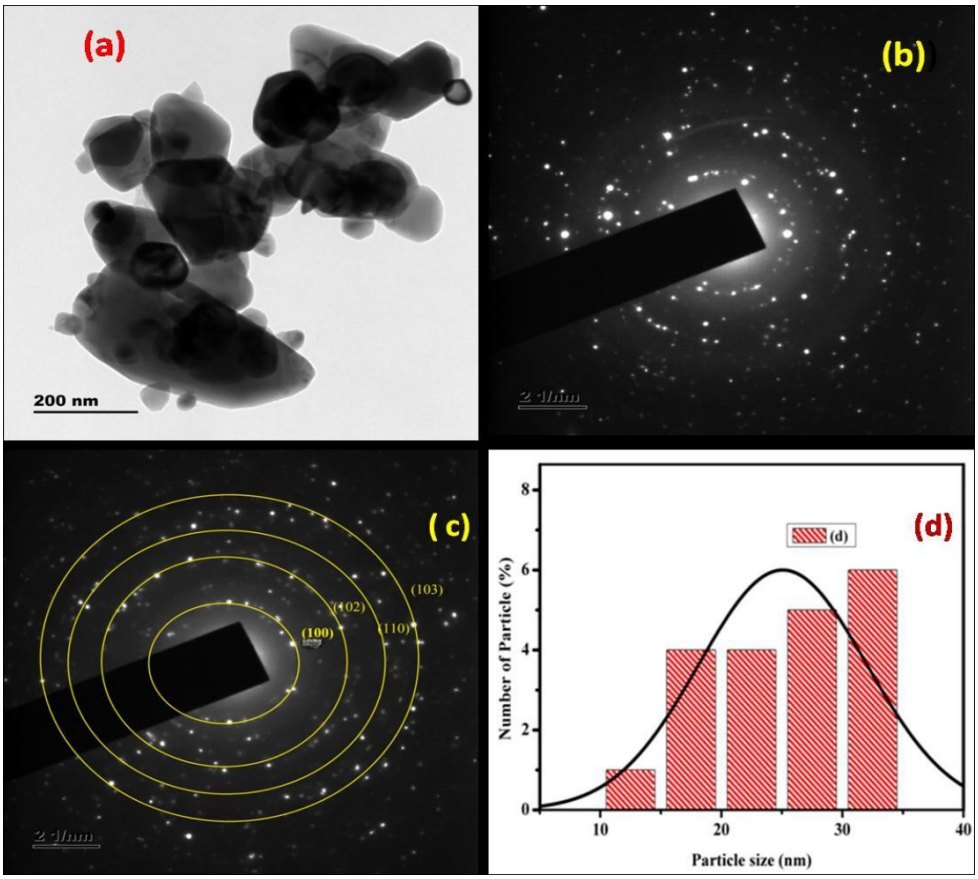

Figure.7. a) HRTEM images b) SAED pattern of ZnO nanopaticles c) SAED pattern with hkl values d) Histogram image

3.4. UV- Visible spectrum analysis

The presence of secondary metabolites in plants facilitates the conversion of zinc ions in solution into zinc oxide, with the plant extract acting as both a reducing and stabilizing agent. This was

confirmed through UV-visible spectroscopy analysis within the wavelength range of 300–800 nm. The UV absorbance peaks for ZnO nanoparticles synthesized using 20 ml, 40 ml, and 60 ml of *Glycosmis pentaphylla* extract were observed at 316.05 nm, 318 nm, and 316.80 nm, respectively (Figure 8), confirming the formation of ZnO nanoparticles.

These results are consistent with earlier reports, where ZnO nanoparticles exhibited absorbance peaks between 310 nm and 360 nm [32, 33]. This phenomenon can be attributed to the "blue shift," wherein a reduction in nanoparticle size leads to a decreased distance between valence bands, thereby increasing the energy and shifting the absorbance wavelength towards the blue region of the spectrum. As a result, ZnO nanoparticles have shorter absorption wavelengths compared to bulk ZnO.Similar absorption maxima within the 340–360 nm range have been reported in previous studies on ZnO nanoparticle synthesis using *Cayratia pedata* leaves [35], as well as extracts from *Cassia fistula* and *Melia azedarach* [36].

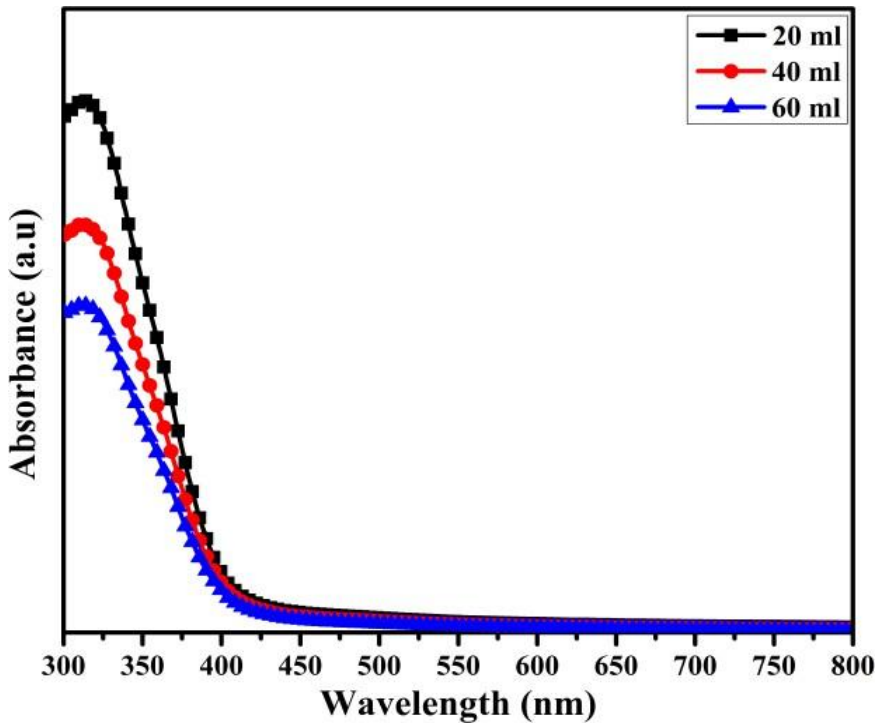

Figure 8. UV–Vis spectral analysis of synthesized ZnO-NPs at different concentrations (20, 40, 60ml) of extract

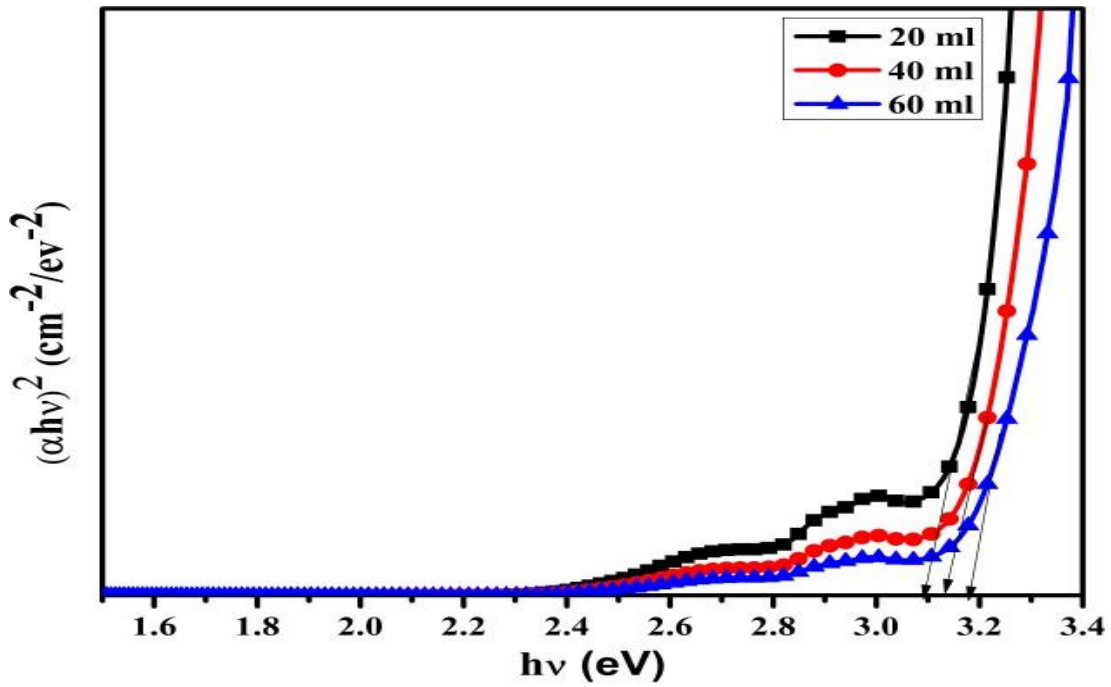

Figure. 9: Bandgap of different concentration of ZnO nanoparticles

Figure 9 shows the bandgap values of prepared ZnO nanoparticles using three variations of extracts. In this figure, the increase of concentration ratio values as increase of bandgap energy values conclude that the higher bandgap values to promote the best activity of antimicrobial and which is good supported with the literature.

3.5. FTIR spectrum analysis

FTIR spectroscopy provides detailed insights into the functional groups responsible for stabilizing, reducing, and capping the nanoparticles. Figure 10 illustrates the FTIR spectra of ZnO nanoparticles synthesized with different extract concentrations (20 ml, 40 ml, and 60 ml). A broad absorption peak was observed at 3432.10 cm^{-1}, 3431.98 cm^{-1}, and 3434.97 cm^{-1} for the 20 ml, 40 ml, and 60 ml extracts, respectively, which is likely associated with the OH stretching vibrations of phenolic compounds.

Peaks at 2927.10 cm^{-1}, 2926.04 cm^{-1}, and 2926.15 cm^{-1} indicate NH bending and CH_3 stretching of alkenes. Moderate peaks appearing at 1630 cm^{-1}, 1645 cm^{-1}, and 1645 cm^{-1} are indicative of carboxylic groups. Sharp peaks at 1091.90 cm^{-1}, 1117.29 cm^{-1}, and 1023.94 cm^{-1} correspond to CO stretching, as well as ester and ether groups in proteins. Additionally, CH phase bending was observed at 779.89 cm^{-1}, 780.88 cm^{-1}, and 780.30 cm^{-1}.

Further peaks at 601.24 cm^{-1}, 618.29 cm^{-1}, and 612.99 cm^{-1} indicate the presence of nitrogen-containing bio-ligands [37]. A distinct vibrational mode for ZnO was identified at 436.75 cm^{-1}, 437.10 cm^{-1}, and 435.38 cm^{-1}, which corresponds to Zn–O stretching bands [38, 39].

These results conclude that the spectrum obtained with the 60 ml extract exhibited sharper peaks, confirming the presence of flavonoids, carboxylic groups, and phenolic compounds in the synthesized sample [40].

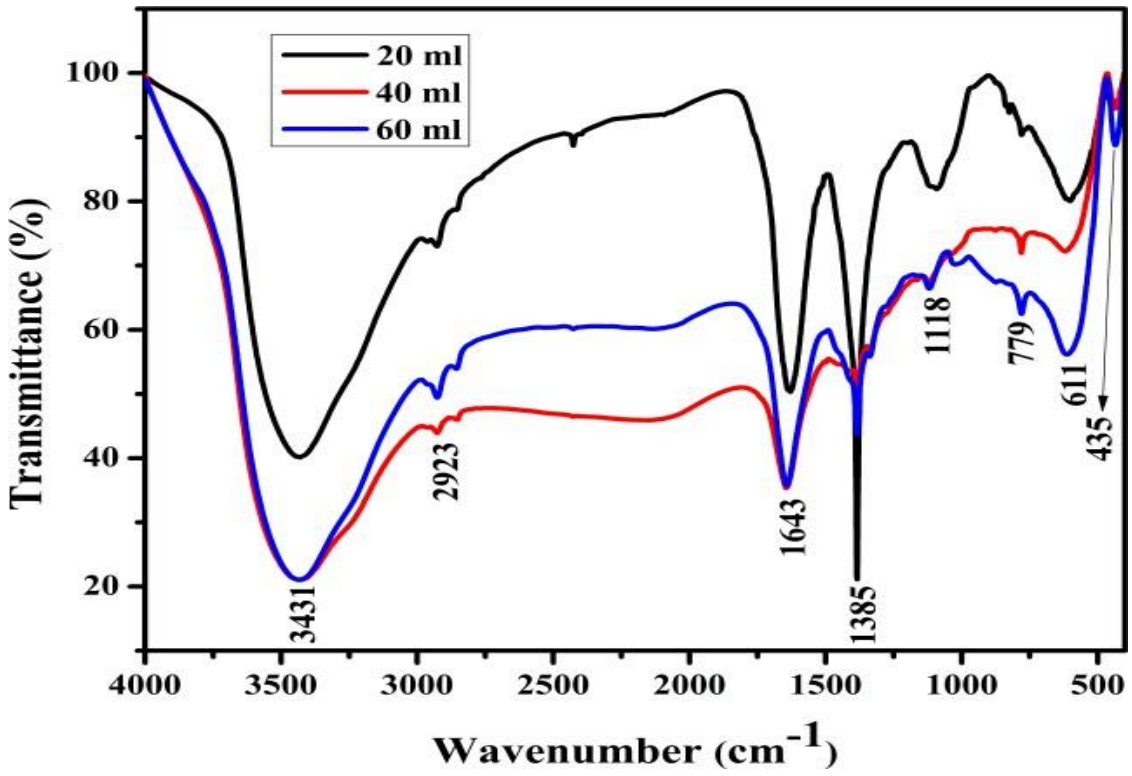

Figure 10. FTIR spectral analyses of synthesized ZnO-NPs at different concentrations (20, 40, 60ml) of extract

3.5. Antimicrobial Activity studies:

3.5.1. Antimicrobial activity of ZnO nanoparticles using plant extract (20ml) against bacterial and fungal strains

The antimicrobial potential of *G. pentaphylla* has been investigated against a range of Gram-negative and Gram-positive bacteria, as well as fungi. The antibacterial properties of ZnO nanoparticles (ZnO-NPs) were assessed qualitatively using agar disc diffusion tests. These tests are effective due to their simplicity, low cost, and ability to screen numerous bacterial strains and antimicrobial agents. The antibacterial mechanism involves disrupting bacterial metabolism, damaging the cell membrane, and inducing oxidative stress, ultimately leading to cell death.

Following incubation, the diameters of the inhibition zones measuring was done. As shown in Figure 11, the inhibition zones for *E. coli* were 1.0 mm, 1.7 mm, and 3.5 mm for ZnO-NP concentrations of 50, 100, and 200 µl, respectively. Similarly, the inhibition zones for *Staphylococcus aureus* were recorded as 0.5 mm, 1.3 mm, and 2.6 mm for the same concentrations (Table and Plate 2). These results indicate that ZnO-NPs exhibit stronger antibacterial activity against Gram-negative bacteria (*E. coli*) compared to Gram-positive bacteria (*Staphylococcus aureus*).

The antifungal activity of ZnO-NPs was also evaluated. The inhibition zones for *Candida albicans* were 0.3 mm, 0.7 mm, and 2.4 mm for ZnO-NP concentrations of 50, 100, and 200 µl, respectively. For *Aspergillus flavus*, the inhibition zones were 0.7 mm, 1.5 mm, and 3.0 mm for the same concentrations. The results indicate that the antimicrobial activity of ZnO-NPs is dose-dependent, with a stronger effect observed at higher concentrations. Among the fungal strains, ZnO-NPs exhibited greater antifungal activity against *Aspergillus flavus* compared to *Candida albicans* (Figure 10) [41–43].

Table 2: Antimicrobial activity of ZnO nanoparticles using plant extract (20ml) against bacterial and fungal strains

S. No.	Microorganisms	Zone of Inhibition (mm in diameter)			
		50µl	100µl	200µl	Standard*
	Bacteria				
1	Escherichia coli	1.00	1.70	3.50	10.00
2	Staphylococcus aureus	0.50	1.30	2.60	10.10
	Fungi				
1	Candida albicans	0.30	0.70	2.40	8.80
2	Aspergillus flavus	0.70	1.50	3.00	9.20

Standard* (Bacteria: Chloramphenicol and Fungi: Fluconazole)

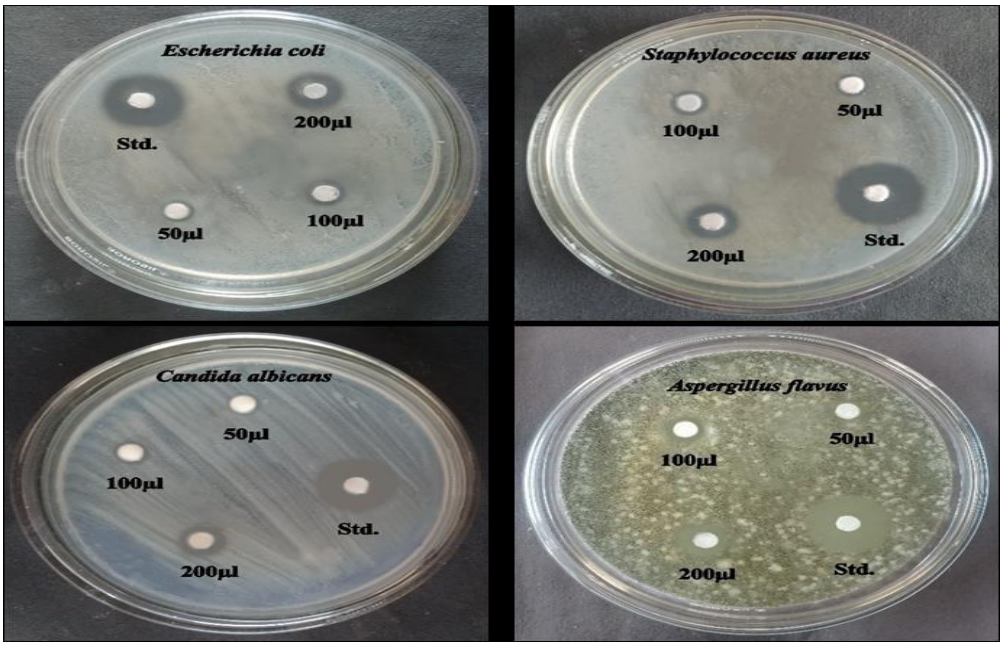

Figure 11: Antimicrobial activity of ZnO nanoparticles using plant extract (20ml) against bacterial and fungal strains

The inhibition zones were measured after incubating 40ml of the solution, with results recorded for E. coli as 2 mm, 2 mm, and 6.70 mm for 50 µl, 100 µl, and 200 µl, respectively (as shown in Fig. 12). For Staphylococcus aureus, the inhibition zones were observed to be 1.30 mm, 2.10 mm, and 4 mm for the same concentrations of 50 µl, 100 µl, and 200 µl, respectively, as presented in Table 3. Among the two bacterial strains, ZnO nanoparticles (ZnO-NPs) exhibited stronger antibacterial activity against the gram-negative bacteria E. coli compared to the gram-positive Staphylococcus aureus.

For fungal strains, antifungal activity was noted through inhibition zones, with Candida albicans showing zones of 0.9 mm, 1.90 mm, and 3.60 mm for 50 µl, 100 µl, and 200 µl, respectively. Aspergillus flavus exhibited inhibition zones of 1.60 mm, 2.80 mm, and 4.30 mm for the same concentrations. The antimicrobial activity was found to increase in a dose-dependent manner. Among the two fungal strains, ZnO-NPs displayed more effective activity against Aspergillus flavus than Candida albicans.

Table 3: Antimicrobial activity of ZnO nanoparticles using plant extract Glycosmis pentaphylla(40ml) against bacterial and fungi strains

S. No.	Microorganisms	Zone of Inhibition (mm in diameter)			
		50µl	100µl	200µl	Standard*
	Bacteria				
1	Escherichia coli	2.00	3.00	6.70	10.10
2	Staphylococcus aureus	1.30	2.10	4.00	9.80
	Fungi				
1	Candida albicans	0.90	1.90	3.60	9.00
2	Aspergillus flavus	1.60	2.80	4.30	9.50

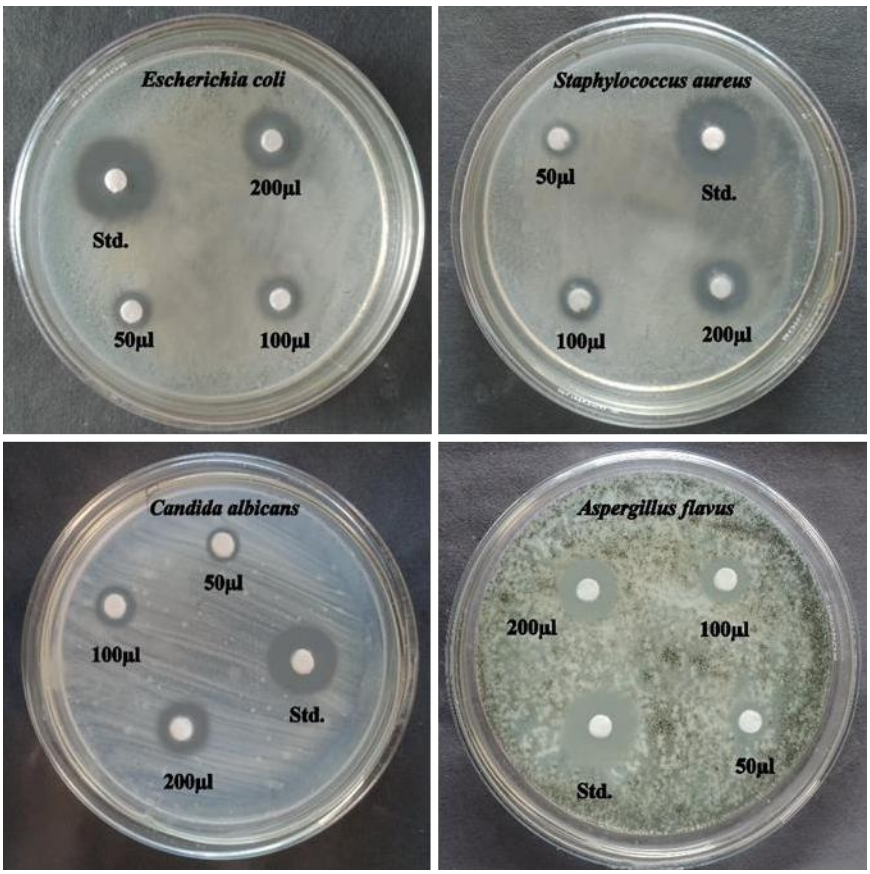

Figure12: Antimicrobial activity of ZnO nanoparticles using plant extract Glycosmispentaphylla(40ml) against bacterial and fungal strains

In the 60ml concentration, inhibition zones were measured after incubation. For *E. coli*, the inhibition zones were recorded as 3.8 mm, 5.9 mm, and 8.60 mm for 50 µl, 100 µl, and 200 µl, respectively (shown in Fig. 13). Similarly, for *Staphylococcus aureus*, the inhibition zones were observed to be 2.20 mm, 3 mm, and 5.10 mm for 50 µl, 100 µl, and 200 µl, respectively, as detailed in Table and Plate 4. Among the two bacterial strains, ZnO nanoparticles (ZnO-NPs) demonstrated stronger antibacterial activity against the gram-negative *E. coli* compared to the gram-positive *Staphylococcus aureus*.

Regarding antifungal activity, inhibition zones for *Candida albicans* were found to be 1.80 mm, 2.60 mm, and 4.80 mm for 50 µl, 100 µl, and 200 µl, respectively. For *Aspergillus flavus*, inhibition zones were measured at 2.70 mm, 3.50 mm, and 5.60 mm for the same concentrations. The antimicrobial activity was observed to increase in a dose-dependent manner. Among the two fungal strains, ZnO-NPs exhibited more effective activity against *Aspergillus flavus* than *Candida albicans*.

From these results, it can be concluded that the increasing concentration of Glycosmis pentaphylla extract enhances the inhibition zone, with the most significant effect on *E. coli* at 200 µl (8.60 mm) compared to *Aspergillus flavus* (5.60 mm). These findings suggest that ZnO nanoparticles have strong antimicrobial properties, and higher concentrations may be effective in treating various diseases.

Table 4: Antimicrobial activity of ZnO nanoparticles using plant extract Glycosmispentaphylla(60ml) against bacterial and fungal strains

S. No.	Microorganisms	Zone of Inhibition (mm in diameter)			
		50µl	100µl	200µl	Standard*
	Bacteria				
1	Escherichia coli	3.80	5.90	8.60	10.20
2	Staphylococcus aureus	2.20	3.00	5.10	9.50
	Fungi				
1	Candida albicans	1.80	2.60	4.80	8.90
2	Aspergillus flavus	2.70	3.50	5.60	9.70

Standard* (Bacteria: Chloramphenicol and Fungi: Fluconazole)

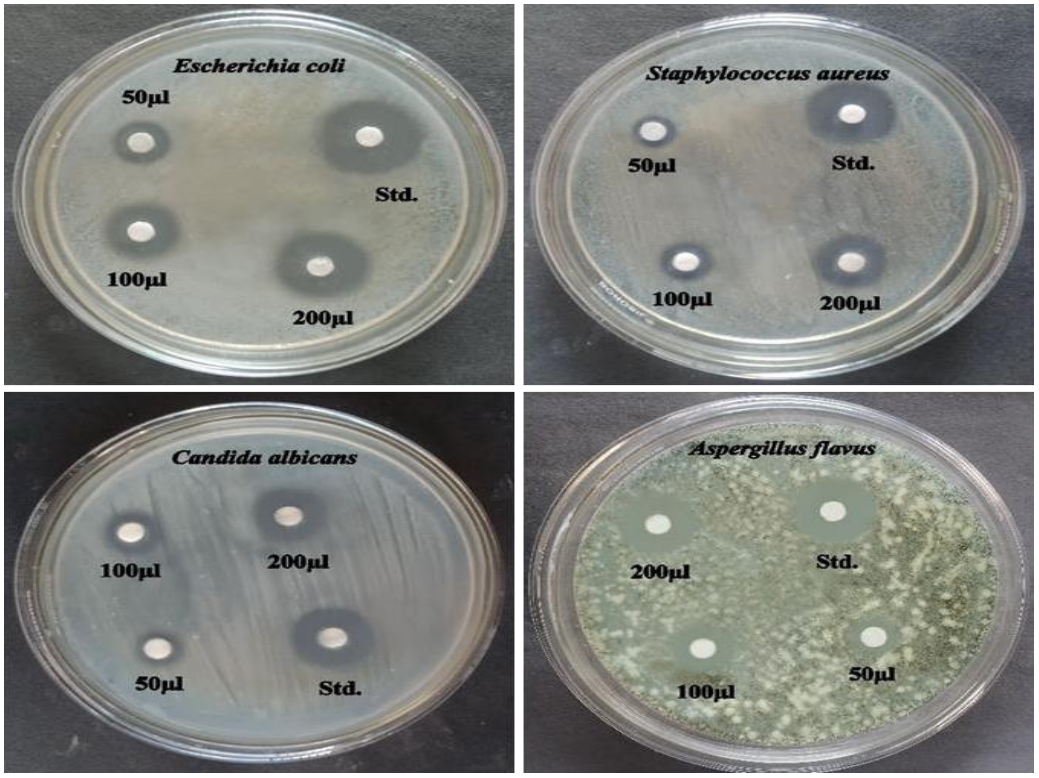

Figure 13: Antimicrobial activity of ZnO nanoparticles using plant extract Glycosmis pentaphylla(60ml) against bacteria and fungal strains

Conclusion:

The co-precipitation method used for synthesizing ZnO nanoparticles (ZnO NPs) with Glycosmis pentaphylla extracts is an environmentally friendly and cost-effective approach. The findings of this study indicate that the tested pathogenic strains are susceptible to ZnO nanoparticles, demonstrating the potential efficacy of these nanoparticles against specific bacterial and fungal strains. This suggests the possibility of expanding the application of ZnO NPs in the biomedical field. X-ray diffraction (XRD) analysis confirmed the presence of ZnO nanoparticles in the prepared sample, while scanning electron microscopy (SEM) supported these results by revealing the morphology of the nanoparticles. Fourier-transform infrared (FT-IR) spectroscopy identified the functional groups of both the ZnO and plant-based components, while the UV-visible spectra showed a peak below 285 nm, indicating the presence of metal oxide. The antimicrobial tests revealed that the synthesized ZnO nanoparticles exhibited strong antibacterial activity against both the bacterial and fungal species tested. Higher inhibition zones were observed, indicating the potential of these nanoparticles to address pathogenic issues, suggesting that the plant-derived ZnO NPs could be useful in mitigating certain diseases.

Acknowledgement

We grateful thanks to Hindusthan College of Arts and Science, and Bharathiyar University, Coimbatore for their research related support to carry out this work.

Funding

The authors declare that no funds, grants, or other any support were received during the preparation of this manuscript.

Data availability

The datasets generated during and/or analyzed during the current study are available from the corresponding author on reasonable request.

Declarations

The authors have no competing interests to declare that are relevant to the content of this article.

References

[1] Desselberger, U. (2000). Emerging and re-emerging infectious diseases. Journal ofInfection, 40(1), 3-15. https://doi.org/10.1053/jinf.1999.0624

[2] Eisenberg, E., & Suzan, E. (2014). Drug combinations in the treatment of neuropathic pain. Current pain and headache reports, 18, 1-8.https://doi.org/10.1007/s11916-014-0463-y

[3] Sawai, J. (2003). Quantitative evaluation of antibacterial activities of metallic oxide powders (ZnO, MgO and CaO) by conductimetric assay. Journal of microbiological methods, 54(2), 177-182.https://doi.org/10.1016/S0167-7012(03)00037-X

[4] Cambon, K., Hansen, S. M., Venero, C., Herrero, A. I., Skibo, G., Berezin, V& Sandi, C. (2004). A synthetic neural cell adhesion molecule mimetic peptide promotes synaptogenesis, enhances presynaptic function, and facilitates memory consolidation. Journal of Neuroscience, 24(17), 4197-4204.https://doi.org/10.1523/JNEUROSCI.0436-04.2004

[5] Darus, M. M., &Mahusin, W. N. (2017, May). Green synthesis of Ag nanoparticles for water treatment (antimicrobial on Eschirichia coli). In AIP Conference Proceedings (Vol. 1847, No. 1). AIP Publishing.https://doi.org/10.1063/1.4983912

[6] Roselli, M., Finamore, A., Garaguso, I., Britti, M. S., &Mengheri, E. (2003). Zinc oxide protects cultured enterocytes from the damage induced by Escherichia coli. The Journal of nutrition, 133(12), 4077-4082.https://doi.org/10.1093/jn/133.12.4077

[7] Brayner, R., Ferrari-Iliou, R., Brivois, N., Djediat, S., Benedetti, M. F., &Fiévet, F. (2006). Toxicological impact studies based on Escherichia coli bacteria in ultrafine ZnO nanoparticles colloidal medium. Nano letters, 6(4), 866-870. https://doi.org/10.1021/nl052326h

[8] Hanley, C., Layne, J., Punnoose, A., Reddy, K., Coombs, I., Coombs, A., ... & Wingett, D. (2008). Preferential killing of cancer cells and activated human T cells using ZnOnanoparticles. Nanotechnology, 19(29), 295103.https://doi.org/10.1088/0957-4484/19/29/295103

[9] Reddy, N. K., Ahsanulhaq, Q., Kim, J. H., Devika, M., & Hahn, Y. B. (2007). Selection of non-alloyed ohmic contacts for ZnOnanostructure based devices. Nanotechnology, 18(44), 445710.https://doi.org/10.1088/0957-4484/18/44/445710

[10] Krishnamoorthy, K., Veerapandian, M., Zhang, L. H., Yun, K., & Kim, S. J. (2012). Antibacterial efficiency of graphene nanosheets against pathogenic bacteria via lipid peroxidation. The journal of physical chemistry C, 116(32), 17280-17287.https://doi.org/10.1088/0957-4484/18/44/445710

[11] Applerot, G., Abu-Mukh, R., Irzh, A., Charmet, J., Keppner, H., Laux, E., & Gedanken, A. (2010). Decorating parylene-coated glass with ZnO nanoparticles for antibacterial applications: a comparative study of sonochemical, microwave, and microwave-plasma coating routes. ACS Applied Materials & Interfaces, 2(4), 1052-1059. https://doi.org/10.1021/am900825h

[12] Salem, W., Leitner, D. R., Zingl, F. G., Schratter, G., Prassl, R., Goessler, W., ...& Schild, S. (2015). Antibacterial activity of silver and zinc nanoparticles against Vibrio cholerae and enterotoxic Escherichia coli. International journal of medical microbiology, 305(1), 85-95.https://doi.org/10.1016/j.ijmm.2014.11.005

[13] Esakki, E. S., Sheeba, N. L., & Sundar, S. M. (2022). Fabrication of dye-sensitised solar cells using four natural sensitisers of ZnO nanoparticle at different pH values. International Journal of Renewable Energy Technology, 13(4), 321-340.https://doi.org/10.1504/IJRET.2022.126467

[14] Jeeva, K., Thiyagarajan, M., Elangovan, V., Geetha, N., & Venkatachalam, P. (2014). Caesalpiniacoriaria leaf extracts mediated biosynthesis of metallic silver nanoparticles and their antibacterial activity against clinically isolated pathogens. Industrial Crops and Products, 52, 714-720.https://doi.org/10.1016/j.indcrop.2013.11.037

[15] Higgins, D. C., Hoque, M. A., Hassan, F., Choi, J. Y., Kim, B., & Chen, Z. (2014). Oxygen reduction on graphene–carbon nanotube composites doped sequentially with nitrogen and sulfur. Acs Catalysis, 4(8), 2734-2740.https://doi.org/10.1021/cs5003806